Appl. Phys. B 37, 159–164 (1985)

Applied Physics B Photophysics and Laser Chemistry

© Springer-Verlag 1985

Injection Locking of ArF Excimer Lasers

A. C. Cefalas and T. A. King

Physics Department, Schuster Laboratory, University of Manchester, Manchester M13 9PL, UK

Received 28 November 1984/Accepted 16 February 1985

Abstract. Injection-locking characteristics of an ArF excimer oscillator-amplifier laser are described including the use of stable-unstable optical cavities. Output intensities of 1 MW cm^{-2} have been produced with 3 mJ output energy, a spectral linewidth better than 5×10^{-3} nm and an injection locking efficiency of 0.9.

PACS: 42.55H, 42.60

The laser pulse from an ArF excimer laser has a broad spectrum due to the bound-to-free dipole transition. The fluorescence spectrum for the ArF molecule is ~3 nm wide (FWHM). Tuning of the excimer lasers is usually achieved with prisms and gratings using the same methods as for several other laser sources. Line narrowed and tunable radiation from excimer sources has a great deal of interest for their use in a variety of applications in photochemistry, spectroscopy and nonlinear optics.

Loree et al. [1], with the use of two prisms inside the laser cavity, achieved pulses with a bandwidth less than 0.2 nm for a KrF laser and 0.05 nm for an ArF laser over a 2 nm tuning range. An ArF excimer laser source with high spectral quality of the laser beam has been described by Egger et al. [2], with 30 mJ output energy, spectral width 10^{-5} nm and with absolute frequency control within 1.8 GHz using a system with 5 amplification stages. Output energies of 125 mJ per pulse at 193 nm have been reported with a tunability better than 2 cm^{-1} by injecting into two excimer lasers the fourth anti-Stokes line of a frequency doubled dye laser in an ArF excimer amplifier system [3]. An ArF excimer laser having a spectral width of 0.002 nm has been reported by Gower [4] using stimulated Brillouin scattering to produce phase conjugate wavefronts. Two prisms and two etalons have been used [5] to produce a linewidth of 0.25 cm^{-1} from ArF.

However, the above methods of tuning usually used more than one tuning element in the laser cavity and the alignment and synchronization of such systems is difficult. The output energy of the laser beam from the oscillator was very weak when a grating at grazing incidence was used as a tuning element. Hence amplification of the laser output from the oscillator was necessary with a second excimer laser and this has been done with the use of the injection locking techniques [6]. Injection locking has been used extensively with excimer lasers for the generation of narrow bandwidth high power ultra-violet radiation with KrF amplifiers at 248 nm [7–9], XeF at 351 nm [10], and XeCl at 308 nm [11–13].

In this paper we report the generation of coherent uv laser radiation at 193 nm with narrow bandwidth 5×10^{-3} nm and an output intensity of 1 MW cm^{-2} using an oscillator-amplifier system in the injection-locking configuration.

1. Experimental

The experimental arrangement is indicated in Fig. 1. The output beam from an ArF oscillator is tuned with a grating at grazing incidence and the narrow-line signal is injected into an amplifier having a stable-unstable optical cavity. Because of the very short radiative lifetime [14] of the bound-to-free transition of the ArF excimer molecule ~4 ns and the short optimum gain time of the laser the time synchronization of the lasers has to be within 1 ns. This can be achieved with an extra spark gap charged at high voltage. The oscillator used an LC-inversion circuit with separate preionization [15, 16] to excite a discharge volume of 80 cm × 2 cm × 0.5 cm. The output energy of the oscillator with no tuning elements or pinholes in the cavity was 30 mJ at 25 kV charging

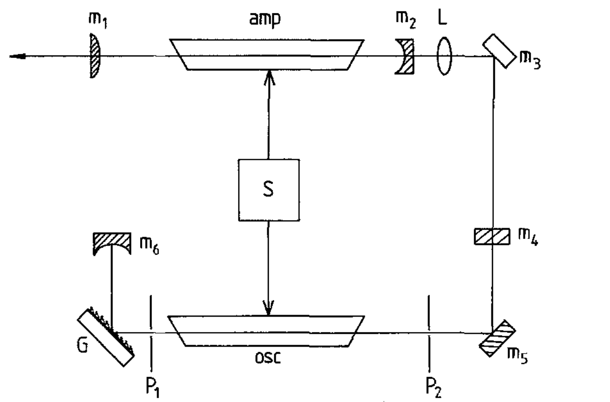

Fig. 1. Injection locking experiment at 193 nm. (m: mirrors, P: pinholes, G: grating, L: lens, S: synchronization circuit of the oscillator and the amplifier)

voltage; the optical cavity had a 3 m radius back mirror (85% reflectivity) and a flat output coupler (10% reflectivity) as the front mirror. The amplifier also used an LC-inversion circuit built inside the laser tube [17]. Using the same optical cavity as for the oscillator the output energy of the laser pulse was 50 mJ at 22 kV charging voltage and 60 cm × 2 cm × 0.5 cm discharge volume.

Synchronization of the lasers was achieved with a trigger circuit having a N_2 spark gap (SG) as the trigger element, as shown in Fig. 2. A trigger signal initially activates the preionization circuit of the oscillator. A portion of the discharge signal of the preionization circuit after a delay of 400 ns is transferred through a high voltage cable to the trigger pin of the spark gap of the preionization circuit of the amplifier. Part of the signal from the discharge of the preionization circuit of the amplifier after a delay activates the spark gap of the trigger circuit (Fig. 2). This spark gap transfers the charge of capacitors in parallel to the trigger pins of the main discharge spark gaps of the two lasers. With this method the two lasers can fire simultaneously with an appropriate delay time introduced by the optical path and the length of the high voltage transfer cables. The capacitance of the transfer cables is $C=100$ pFm^{-1}, with total $C_2 \approx 200$ pF and inductance $L_2 = 250$ nHm^{-1}. The equivalent circuit which takes into account the inductance and the capacitance of the transfer cables is as in Fig. 2. The pin of the spark gap of the main discharge is connected in parallel with the capacitance C_2 of the cable, so that the voltage across the capacitance C_2 will be the voltage across the trigger pin of the spark gaps of the main discharge circuits $V(t)$.

The circuit analysis of Fig. 2 gives the voltage $V(t)$ across the trigger pin of SG (Fig. 2) and earth as

$$V(t) = V_0 \frac{C_1}{C_2 + C_1} \frac{\omega^2}{\omega^2 + a^2} \cdot \left[\exp(-at) - \frac{a}{\omega} \sin(\omega t) - \cos(\omega t) \right] \tag{1}$$

with

$$\omega = (L_2 C_2)^{-1} . \tag{2}$$

The value of $1/a$ determines the rise time of the voltage across the trigger pin of the spark gap. The spark gap will be triggered when the voltage $V(t)$ reaches its breakdown value V_b at time t_b. The distance between the firing pin and the electrode of the spark gap is 0.2 mm and the value of the breakdown voltage at 3 atm N_2 pressure is 1000 V. For $a = 2 \times 10^8$ s^{-1} and $\omega = 1.5 \times 10^8$ s^{-1} and at 25 kV charging voltage V_0 we get $t_b = 0.5$ ns. Then the jitter in the firing time between the two spark gaps is expected to be of the same order of magnitude. So the overall jitter is determined by the jitter between the discharge voltage across the electrodes of the lasers and the laser pulse which is $\simeq 1$ ns.

The divergence of the laser beam for a stable cavity configuration was 5 mrad and the beam cross section,

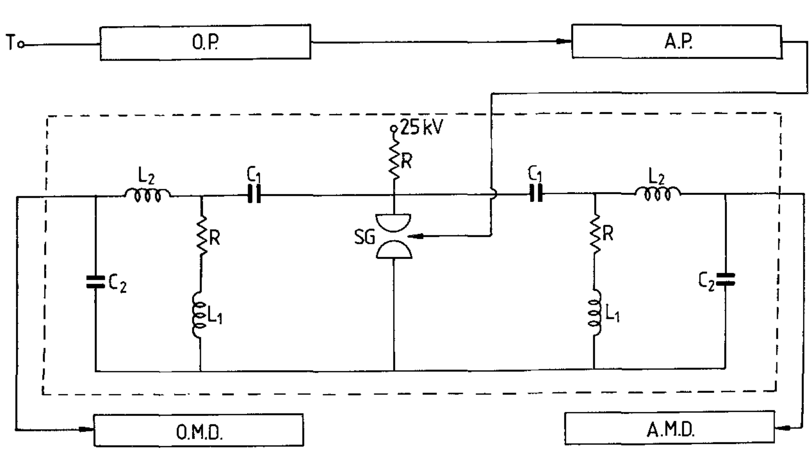

Fig. 2. Synchronization circuit. (T: trigger, O.P: preionization circuit of the oscillator, A.P: preionization circuit of the amplifier, SG: spark gap, OMD: main discharge circuit of the oscillator, AMD: main discharge circuit of the amplifier)

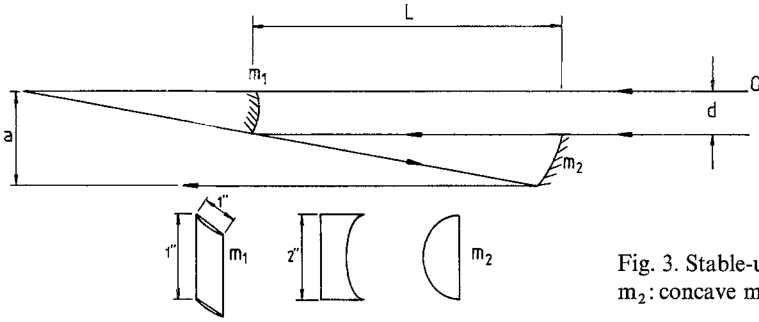

Fig. 3. Stable-unstable optical cavity (m_1: cylindrical mirror, m_2: concave mirror)

when focused with a 50 cm lens, had a spot size of $1 \times 0.5\,mm^2$. The focusing properties of the beam can be improved with the use of an unstable cavity. For nonlinear optical experiments [19] in order to avoid the central hole in the near field of the amplified laser beam with the unstable cavity configuration a stable-unstable cavity [18] was formed with a cylindrical and a concave mirror (Fig. 3). The magnification M of the cavity is given by

$$M=\frac{R_2}{R_1}, \tag{3}$$

where R_2 and R_1 are the radii of curvature of the concave and the cylindrical mirrors, respectively, and are equal to 275 and 13 cm.
The distance L between the mirrors is

$$2L=R_2-R_1. \tag{4}$$

The distance d into which the cylindrical mirror was projected into the discharge region is given by the equation

$$d \cdot M=a, \tag{5}$$

where a is the laser electrode spacing. For $a=20$ mm and $M=21$ then $d=0.95$ mm. The small value of distance d can create serious alignment problems but the choice of the magnification M has to be high because the above value allows a diffraction limited beam to become the predominant mode [9]. Precise alignment of the system has to be carried out in the xyz directions and a micrometer alignment system has been designed for this purpose. The output energy of the resonator in the unstable-stable configuration was 20 mJ at 2 kV charging voltage. The divergence of the beam was 0.3 mrad in the unstable plane and the beam can be focused down to spot sizes less than 0.1 mm.

2. Performance of the System

The oscillator was tuned with a grating at grazing incidence having a ruled area of 25 cm × 25 cm. The total number of diffraction grooves over this area is 30480 and the theoretical resolution of the grating is 6×10^{-3} nm in the first order. Mode control was achieved with one front and one back circular pinhole, each having a diameter of 0.4 mm. The grating resolution is a function of the incident angle of the radiation onto the grating, with the grating at an angle of 82° and in the fourth order it is 5×10^{-5} nm. The energy of the tuned radiation with the grating at 85° in various orders is indicated in Fig. 4. The maximum measured resolution of the tuned laser radiation was limited by the resolution of the monochromator to 0.005 nm. The detected output tuned signal reduced with increasing incidence angle and disappears for an angle greater than 88°. The output signal with angle of incidence is indicated in Fig. 5. The laser can be tuned from 192.5 to 193.6 nm with the tuned radiation having an energy of 20 µJ. The spectrum of the tuned laser pulse is indicated in Fig. 6a and b for two positions of the tuning element. The background noise of the tuned signal is due to the low reflectivity of the front mirror M5 and significant reduction of the noise is expected with a higher reflectivity front mirror. The tuned output of the oscillator was injected into the amplifier, as in Fig. 3, from the back of the mirror M_2, with a lens focusing the injected signal onto the cylindrical mirror.

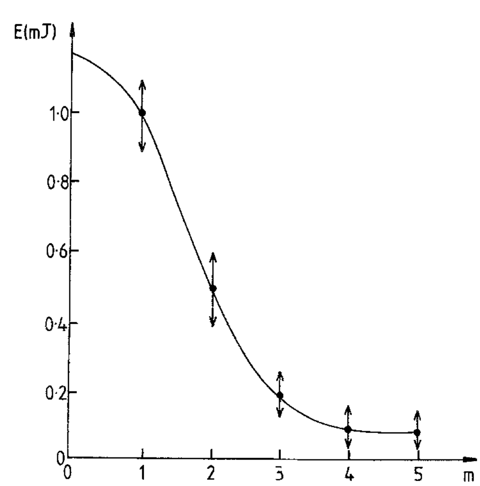

Fig. 4. Output energy from the oscillator with different diffraction order m

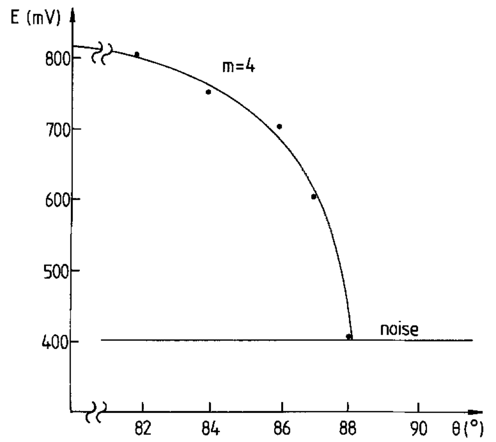

Fig. 5. Output energy from the oscillator in fourth order with the diffraction angle

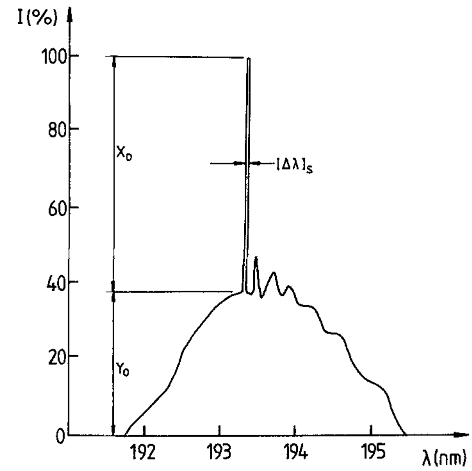

Fig. 7. Injection locked signal. Taken with monochromator resolution $<5\times10^{-3}$ nm, Tektronix 7904 and 1 Hz repetition rate

We define the efficiency η of the injection locking as the ratio of the signal intensity x_0 to the total intensity x_0+y_0. The efficiency of the injection locking increases with increasing spectral quality. For the ideal case, when the background noise is negligible, $\eta=1$. With careful alignment of the system the efficiency can be 0.6, but this value is subject to variations. A more realistic value for the experiment, which is independent of wavelength, is $\eta=0.4$. The energy of the laser pulse (signal) is now 2 mJ and the spectral linewidth is less than 5×10^{-3} nm. The mean value of the output intensity of the laser pulse is $1\,\mathrm{MW\cdot cm^{-2}}$. The efficiency of the injection locking can be evaluated from the spectrum. The efficiency for grazing angles below 80° becomes zero and injection locking takes place only for injection signals with good spectral quality.

For a given grating angle and a given charging voltage for the oscillator and the amplifier the efficiency depends on the alignment of the cylindrical mirror and the back concave mirror. The efficiency drops by 50% when the mirrors are misaligned by 0.5 mrad. The effect of the injected signal on the amplifier is very clear, the spectrum of the output from the unstable resonator

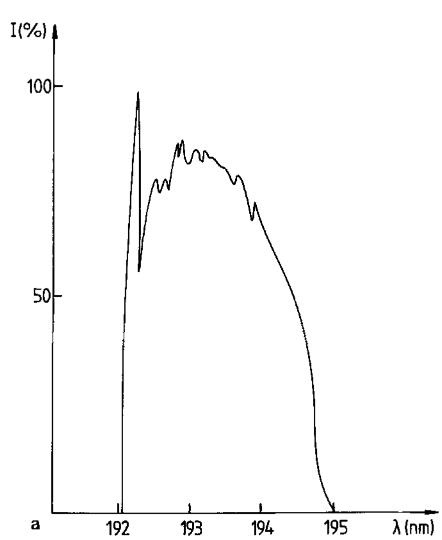

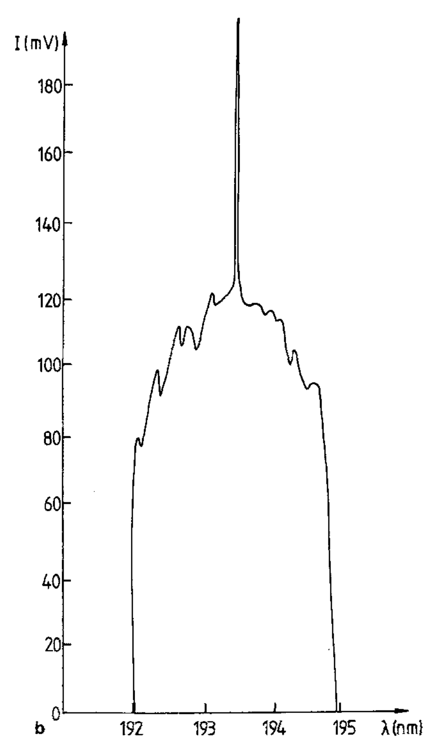

Fig. 6a and b. Tuning of the oscillator, (a) linewidth edge, (b) linewidth centre

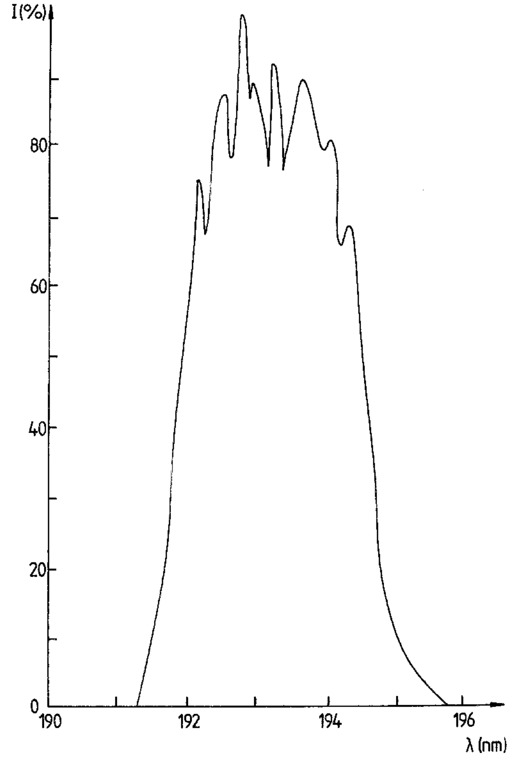

Fig. 8. Spectrum of the ArF excimer without injection loking

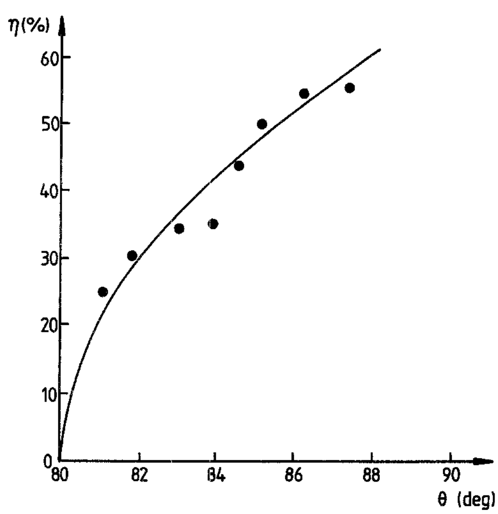

Fig. 9. Spectral efficiency with grazing angle

when the injected signal is blocked is completely changed, as shown in Fig. 8. During the execution of the above experiments there were cases where the efficiency of the above experiment was 90%. Obviously the efficiency of the injection locking depends on the proper alignment of the system and when the injected beam traces the whole discharge volume the efficiency should be optimum, but such spatial control is very difficult in practice.

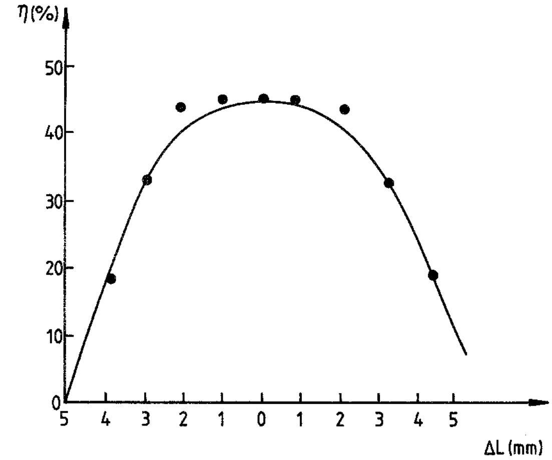

Fig. 10. Spectral efficiency with the misalignment of the optical cavity

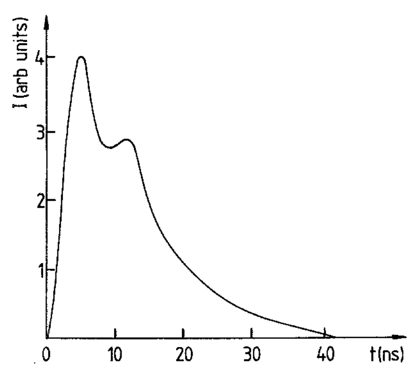

Fig. 11. Temporal evolution of the locked pulse

Figure 9 shows the efficiency of the cavity with the grazing angle of the grating of the oscillator and in Fig. 10 the efficiency of injection locking is shown with the misalignment distance $\Delta L = 0.5$ cm and this result indicates the high sensitivity of the locking on the alignment of the optical cavity. The temporal evolution of the pulse in the case of successful injection locking is indicated in Fig. 11 when a mode competition effect is now apparent. The mode beating disappears in the case of no injection locking (Fig. 12) and is a quick way to check the operation of the system. The mode beating effect occurs only around the central injected frequency and disappears at neighbouring frequencies.

3. Summary

An injection locked ArF excimer system at 193 nm has been designed having a stable-unstable optical cavity formed by a cylindrical front mirror and a concave back mirror. With this method the near field pattern does not have a central hole and the beam is suitable for amplification in, for example, nonlinear optics

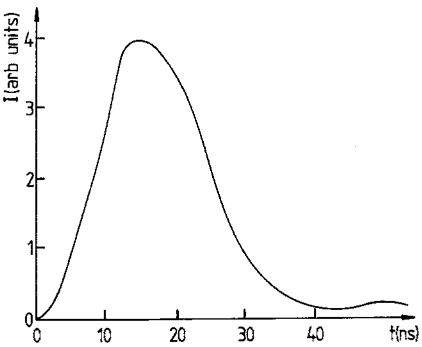

Fig. 12. Temporal evolution of the unlocked pulse

experiments. The spectral linewidth of the beam was better than 5×10^{-3} nm and the intensity of the beam after focusing with a 2 m focal lens was 20 MW cm^{-2}.

Acknowledgement. Funding from the Science and Engineering Research Council for part of this work is gratefully acknowledged.

References

1. T.R. Loree, K.B. Butterfield, D.L. Barker: Appl. Phys. Lett. **32**, 171 (1978)
2. H. Egger, T. Srinivasan, K. Hohla, H. Scheingraber, C.R. Vidal, H. Plummer, C. Rhodes: Appl. Phys. Lett. **39**, 37 (1981)
3. J.C. White, J. Bokor, R.R. Freeman, D. Henderson: Opt. Lett. **6**, 293 (1981)
4. M.C. Gower: Opt. Lett. **8**, 70 (1983)
5. R.S. Hargrove, J.A. Paisner: In *Digest of Topical Meeting on Excimer Lasers*, IEEE Cat. No. 79CH1470-4QEA, IEEE, New York (1979)
6. C.J. Buczek, R.J. Freiberg, M.L. Skolnick: Proc. IEEE **61**, 1411 (1973)
   R. Adler: Proc. IEEE **61**, 1380 (1973)
7. J. Goldhar, W.R. Rapoport, J.R. Murray: IEEE J. QE-**16**, 235 (1980)
8. J. Banic, T. Efthimiopoulos, B.P. Stoicheff: Appl. Phys. Lett. **37**, 686 (1980)
9. R.G. Caro, M.C. Gower, C.E. Webb: J. Phys. D **15**, 767 (1982)
10. J. Goldhar, J. Dickie, L.P. Bradley, L.D. Pleasance: Appl. Phys. Lett. **31**, 677 (1977)
    I.J. Bigio, M. Slatkine: Opt. Lett. **6**, 336 (1981)
11. T.J. Pacala, J.B. Laudenslager: Appl. Phys. Lett. **37**, 366 (1980)
12. G. Reksten, T. Varghese, D.J. Bradley: Appl. Phys. Lett. **38**, 513 (1981)
13. Lambda-Physik: Excimer laser model EMG 150
14. C.K. Rhodes (ed.): *Excimer Lasers* 2nd ed., Topics Appl. Phys. **30** (Springer, Berlin, Heidelberg 1984)
15. R. Burnham, N. Djeu: Appl. Phys. Lett. **29**, 707 (1976)
16. S. Watanabe, S. Shiratori, T. Sato, H. Kashiwagi: Appl. Phys. Lett. **33**, 141 (1978)
17. A.C. Cefalas, T.A. King: J. Phys. E **17**, 760 (1984)
18. O.L. Bourne, P.E. Dyer: Opt. Commun. **31**, 193 (1979)
19. A.C. Cefalas, T.A. King: Opt. Commun. **51**, 105 (1984)